Available online at www.sciencedirect.com
ScienceDirect
Deep-Sea Research II 55 (2008) 868–879
DEEP-SEA RESEARCH PART II
www.elsevier.com/locate/dsr2

Mesopelagic organic carbon remineralization in the Kerguelen Plateau region tracked by biogenic particulate Ba

S.H.M. Jacquet[a,*,1], F. Dehairs[a], N. Savoye[a,2], I. Obernosterer[c,d], U. Christaki[e], C. Monnin[f], D. Cardinal[b]

[a]*Analytical and Environmental Chemistry Department, Vrije Universiteit Brussel, Brussels, Belgium*
[b]*Royal Museum for Central Africa, Department of Geology, Tervuren, Belgium*
[c]*CNRS, UMR 7621, LOBB, Observatoire Océanologique, F-66651 Banyuls/mer, France*
[d]*UPMC Univ Paris 06, UMR 7621, LOBB, Observatoire Océanologique, F-66651 Banyuls/mer, France*
[e]*Laboratoire d'Océanologie et de Géosciences – CNRS – UMR LOG 8187, Université du Littoral Côte d'Opale (MREN), 62930 Wimereux, France*
[f]*Laboratoire Mécanismes de Transfert en Géologie, CNRS-Université Paul Sabatier, Toulouse, France*

Accepted 9 December 2007

Abstract

We report on the distribution of excess, non-lithogenic particulate barium (Ba), a proxy for twilight-zone remineralization of organic matter (OM), in the Kerguelen Plateau area during the late austral summer of 2005. This study was part of a broader investigation focusing on natural iron fertilization controlling the characteristic and recurrent phytoplankton blooms in the region. The Plateau area contrasted strongly with the off-shelf HNLC area. Plateau stations had quite high excess of Ba_{xs} contents (up to 5000 pM) in surface waters (upper 150 m) that coincided with enhanced phytoplankton biomass. However, it had a lower mesopelagic (125–450 m) excess of biogenic Ba contents when compared to the off-shelf stations. Particulate excess Ba in the twilight zone (125–450 m depth layer) proved to be significantly set by the vertical distribution of bacterial activity, with higher particulate Ba contents in situations where significant bacterial activity extended deeper in the water column. These observations are in agreement with the role of excess biogenic particulate Ba as a proxy of twilight-zone OM remineralization. Using a transfer function established during earlier work, we calculated organic carbon remineralization rates and weighed these against other carbon fluxes (primary production, bacterial carbon demand), including carbon export from the 125-m horizon (^{234}Th method). Off-shelf HNLC stations had a larger fraction of the organic carbon production exported and subsequently mineralized in the mesopelagic waters (125–450 m). Plateau stations had a smaller fraction of produced carbon exported, but this fraction appeared less prone to remineralization in the twilight zone and therefore had potential to reach the shallow (~500 m) seafloor or to be exported off-shelf. Differences in trophic structure and in composition of the diatom community would explain the variability in twilight-zone remineralization processes and in transfer efficiency through the mesopelagic zone in the Kerguelen Plateau area.

Keywords: Particulate biogenic barium; Mesopelagic remineralization; Iron fertilization; Kerguelen Plateau

1. Introduction

In studying the key role played by the Southern Ocean (S.O.) in the global carbon (C) cycle and climatic changes, efforts have gone into understanding the biological pump through which C fixed by phytoplankton is exported from the surface to the deep ocean. Present day evidence that iron (Fe) limits ocean primary production (PP) in high-nutrient low-chlorophyll (HNLC) regions (Martin, 1990; Martin et al., 1994; Coale et al., 1996) focuses interest on ocean fertilization as a C-sequestration tool. Recent large-scale experiments demonstrated the role of iron in enhancing the S.O. phytoplankton biomass and production (IronEx, SOIREE, EisenEX, SEEDS, SOFeX and EIFEX

*Corresponding author. Tel.: +32 2 629 39 70; fax: +32 2 629 32 74.
E-mail address: jacquet@cerege.fr (S.H.M. Jacquet).
[1]Now at: CEREGE, UMR 6635, Europôle Méditerranéen de l' Arbois, Aix en Provence, France.
[2]Now at: OASU, UMR EPOC, Université Bordeaux 1, CNRS, Station Marine d'Arcachon, Arcachon, France.

0967-0645/$ - see front matter © 2008 Elsevier Ltd. All rights reserved.
doi:10.1016/j.dsr2.2007.12.038

cruises; Boyd et al., 2000, 2004; Gervais et al., 2002; Buesseler et al., 2004, 2005; de Baar et al., 2005; Hoffmann et al., 2006), confirming former phytoplankton incubations (Martin and Fitzwater, 1988; Hutchins and Bruland, 1998; Takeda, 1998). However, determining to what extent fertilization could modify the actual export of sinking particulate organic carbon (POC) to the deep ocean is far from being comprehensively achieved. This is partly due to the short term over which the observations were made, thus precluding extrapolation to longer time scales (Bidigare et al., 1999; Nodder et al., 2001; Trull and Armand, 2001; Nodder and Waite, 2001; Buesseler et al., 2004, 2005; Bishop et al., 2004; Aono et al., 2005; Aumont and Bopp, 2006). Moreover, the magnitude of the export increase is not the only parameter that is important in inferring the degree of C sequestration (Sarmiento et al., 2004). Indeed, the fate of carbon exported under such Fe fertilization experiments is largely overlooked, although remineralization in mesopelagic waters (~100–1000 m; also referred to as the twilight zone) is responsible for the release of most of the carbon exported from the surface mixed layer (ML) (Lampitt and Antia, 1997; Martin et al., 1987; Sarmiento et al., 1993; Suess, 1980). As the mesopelagic zone has all too often been neglected, the efficiency of remineralization processes remains poorly understood today. However, organic matter (OM) processing in the twilight zone is of considerable significance since remineralization length scales are important indicators of the capacity of intermediate layers for longer-term carbon sequestration. The efficiency of the biologic pump in exporting and routing C towards longer-term sequestration is mainly set in these intermediate layers (Longhurst et al., 1990; Boyd et al., 1999; Kriest and Evans, 1999; François et al., 2002; Passow and De La Rocha, 2006; Buesseler et al., 2007; Biddanda and Benner, 1997; Reinthaler et al., 2006). A quantitative representation of this process is thus integral to every simulation of the ocean's role in the global carbon cycle.

Next to the artificial fertilization experiments outlined above, a natural iron-fertilization survey (KEOPS cruise; Kerguelen: Ocean and Plateau compared Study) was conducted during the late austral summer 2005 on the Kerguelen Plateau, southeast of the Kerguelen Islands and northeast of Heard Island (Indian sector of the S.O.). The Kerguelen Plateau is characterized by recurrent and predictable massive blooms (Blain et al., 2001), as sustained by Fe inputs from shelf sediments. During KEOPS, the Kerguelen Plateau thus served as a laboratory to study the effect of natural iron fertilization on ecosystems functioning and C cycling (Blain et al., 2007). Contrasting with short-term artificial Fe experiments, special emphasis was placed on the potential of the Kerguelen Plateau and margin system for deep C sequestration. Therefore, the present work focuses on remineralization of particulate OM in the mesopelagic zone, as assessed from the distribution of excess biogenic particulate barium (Ba_{xs}). Dehairs et al. (1980, 1990, 1991, 1992, 1997) showed that the oceanic mesopelagic Ba_{xs} stock is mainly composed of discrete micron-sized barite ($BaSO_4$) crystals formed in degrading detritus sinking from the surface and released into the water column at the breakdown of the carrier phase (particulate organic materials, biogenic aggregates) (Dehairs et al., 1980, 1992, 1997; Stroobants et al., 1991; Cardinal et al., 2005). This led to use mesopelagic Ba_{xs} as a proxy for remineralization of exported biogenic matter, and recent results of bacterial production (BP) and Ba_{xs} distribution appear to strengthen this (Dehairs et al., in press). Further details on the excess, non-lithogenic particulate Ba proxy are given below.

Here, we examine the mesopelagic (meso-) Ba_{xs} distribution to infer C remineralization at contrasted settings in naturally iron-fertilized waters above the Kerguelen Plateau and off-shelf HNLC waters. The present work is part of a multi-proxy approach targeting the fate of an iron-induced bloom and the associated flux of sinking particles, with the goal being to refine assessments of carbon sequestration by the ocean under natural iron fertilization conditions.

2. Experiment and method

2.1. Sampling and analysis

During the KEOPS cruise in the Kerguelen Plateau region (19 January–13 February 2005; R/V *Marion Dufresne*), eight stations were sampled for particulate barium (Ba_p) along three transects (A, B, and C) crossing the Kerguelen Plateau and extending into the off-shelf deep

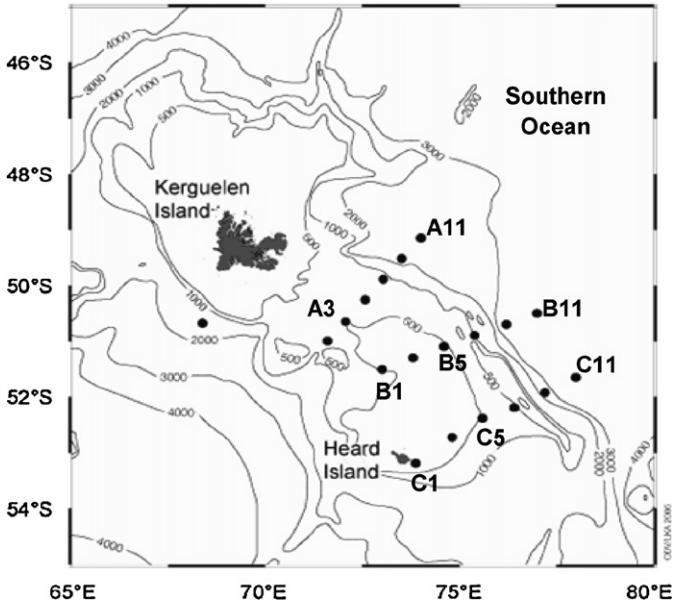

Fig. 1. Map of the Kerguelen Plateau study area showing the three transects A, B, and C with stations' location. Reference station A3 is located on the Plateau in the core of the bloom and station C11 off-shelf in typical HNLC waters.

ocean (Fig. 1). All stations were located south of the Polar Front (PF). Since the bloom in this area appears remarkably constrained by the bathymetry of the Plateau (Blain et al., 2001, 2007) and thus to potential iron supply, the focus during KEOPS was on two contrasting sites in particular—station A3 (located on the Plateau in the core of the bloom; 50.62°S, 72.07°E) and C11 (located off-shelf in typical of HNLC waters; 51.65°S, 78.00°E). A3 and C11 were sampled three times (24/01, 03/02, and 12/02) and two times (26/01 and 5/02), respectively, for Ba_p; the other stations were visited once. Here, the different repeats of A3 and C11 consist of the third, fourth, and fifth visits for A3 (the two first visits of A3 were not sampled for Ba_p), and in the first and second visits for C11, respectively. In the following, we use both the station and CTD numbers to refer to stations.

Sampling of suspended matter was done using a CTD Rosette equipped with 24 12-L Niskin bottles. 4–7 L of seawater were filtered on polycarbonate membranes of 0.4 μm porosity. On board, the filters were dried (50 °C) and stored in petri dishes for later analysis. In the home-based laboratory, samples were digested using an HCl/HNO_3/HF acid mixture and analyzed for Ba and Al. Particulate Al was analyzed by ICP-AES (inductively coupled plasma-atomic emission spectrometry; Thermo Optek Iris Advantage) with an average relative standard error of 14%, while particulate Ba was analyzed by ICP-QMS (inductively coupled plasma-quadrupole mass spectrometry; VG Plasma Quad 2+ Thermo Elemental) with an average relative standard error of 5% (Cardinal et al., 2001). In order to calculate biogenic barium, called excess Ba (Ba_{xs}), total particulate Ba was corrected for lithogenic Ba using Al as a crustal reference (Taylor and McLennan, 1985; Cardinal et al., 2001). At most sites, particulate biogenic Ba_{xs} represented >95% of total particulate Ba. However, lithogenic Ba was particularly high at shallow Plateau stations such as C1–100 (close to Heard Island), representing 78–87% of total particulate Ba (Table 1). At station B5–60 and to a lesser extent station C5–91, lithogenic Ba reached up to 20% of total Ba_p, especially in approach of the seafloor (at 526 and 550 m, respectively). Therefore, we expect that subtracting the lithogenic Ba fraction induced a larger error on the Ba_{xs} numbers at B5 and also at some discrete depths at C1 and C5. At the other stations the lithogenic fraction was very small (<5%), and therefore the impact on the Ba_{xs} precision minimal. The presence of higher lithogenic Ba contribution at stations C1, B5, and C5 on approach of the seafloor could reflect potential sediment redistribution/water mass advection in this zone. This fits with the complex hydrodynamics above the Kerguelen Plateau, reflected for instance by the more vigorous conditions that prevail at the eastern escarpment of the Plateau compared to the shallow Plateau itself (Park et al., 2008a, b), and corroborated by radium isotope data (van Beek et al., 2008). Bottom currents circulating along the shelf break could thus explain the enhanced lithogenic Ba supply at C1, B5, and C5.

2.2. C remineralization fluxes

As outlined above, the mesopelagic (meso-) Ba_{xs} signal, mainly composed of barite micro-crystals ($BaSO_4$; Dehairs et al., 1980) builds up during the phytoplankton growth season as the result of degradation and remineralization of particulate biogenic organic materials exported from the surface (Dehairs et al., 1997; Cardinal et al., 2001, 2005). Observations support that in a world ocean mostly undersaturated with barite (Monnin et al., 1999; Monnin and Cividini, 2006), these biogenic aggregates provide the necessary thermodynamic conditions for barite precipitation during OM remineralization, through sulfate and/or barium enrichment (Dehairs et al., 1980, 2000; Bishop, 1988; Stroobants et al., 1991). The Ba_{xs}–barite water-column distribution reflects production of particulate Ba to take place below the upper ML and to be ongoing in the twilight zone and deeper, as recently emphasized by van Beek et al. (2008).

The remineralized C in the mesopelagic layer was estimated using an algorithm relating meso-Ba_{xs} contents to the rate of oxygen consumption deduced via a 1D advection–diffusion–consumption model applied on highly resolved, precise dissolved O_2 profiles along 6°W in the S.O. (Shopova et al., 1995; Dehairs et al., 1997):

$$J_{O_2} = \frac{(\text{meso}Ba_{xs} - Ba_{residual})}{17\,200} \quad (1)$$

$$C_{respired} = Z \times J_{O_2} \times RR \quad (2)$$

where J_{O_2} is the O_2 consumption (μmol L^{-1} d^{-1}), $C_{respired}$ is the carbon mineralized rate (in mmol C m^{-2} d^{-1}; further expressed in mg C m^{-2} d^{-1}), Z is the thickness of the depth layer over which meso-Ba_{xs} is calculated, RR is the stoichiometric C:O_2 mole ratio (127:175; Broecker et al., 1985), meso-Ba_{xs} is the Ba_{xs} amount that accumulates over the growth season, and $Ba_{residual}$ is the background Ba_{xs} signal at zero oxygen consumption, i.e. zero organic C demand. The residual Ba_{xs} likely depends on the saturation state of the water with respect to barite. For the S.O. south of the PF, shown by to be saturated for pure $BaSO_4$ (Monnin et al., 1999) and (Ba,Sr)SO_4 solid solutions (Monnin and Cividini, 2006) from surface to 2500 m, this residual Ba_{xs} is close to 180 pM (Dehairs et al., 1997). During KEOPS, saturation index (SI) calculations confirmed that the upper mesopelagic water column (125–450 m) throughout the study area is in equilibrium with pure barite (0.9<SI<1.1) (Fig. 2A). Surface waters (upper 125 m) as well were generally saturated, though some discrete depths at Plateau and margin stations showed undersaturation (Fig. 2A). The latter condition is driven by lower dissolved Ba concentrations at these depths. Below 2000–2500 m SI values for KEOPS show that the water column becomes undersaturated for $BaSO_4$, (Fig. 2B) as reported also for the Circumpolar Ocean elsewhere (Monnin et al., 1999). A residual Ba_{xs} value of 180 pM is close to the average Ba_{xs} contents observed at

Table 1
Excess particulate Ba (Ba_{xs}; pM) and particulate Al (nM) at KEOPS stations. Ba_{xs} [%] represents the non-lithogenic fraction of the total particulate Ba signal

A3–32 (seafloor: 525 m)					A3–73 (seafloor: 525 m)					A3–119 (seafloor: 525 m)					A11–11 (seafloor: 2600 m)				
Niskin	Depth [m]	Ba_{xs} [pM]	Ba_{xs} [%]	Al [nM]	Niskin	Depth [m]	Ba_{xs} [pM]	Ba_{xs} [%]	Al [nM]	Niskin	Depth [m]	Ba_{xs} [pM]	Ba_{xs} [%]	Al [nM]	Niskin	Depth [m]	Ba_{xs} [pM]	Ba_{xs} [%]	Al [nM]
Transect A																			
22	10	576	95	21.9	24	10	2800	100	5.5	23	12	517	98	6.1	24	8	59	86	7.2
20	31	142	90	11.9	21	50	5930	100	4.6	21	30	1766	100	4.4	23	30	272	96	9.2
18	50	1355	98	20.3	20	74	5814	100	3.4	19	51	2638	100	8.3	21	76	152	91	11.1
16	74	557	99	5.8	18	99	2249	99	17.3	17	75	4115	100	8.1	20	101	99	89	9.5
14	100	436	97	8.3	17	125	3213	99	12.4	14	101	2826	99	11.1	19	125	267	95	10.8
12	124	274	96	8.4	15	150	269	96	8.2	11	150	287	98	4.5	18	150	546	91	40.3
10	150	408	96	13.9	14	199	330	99	3.2	9	200	255	97	6.7	17	199	146	93	7.7
8	199	190	94	9.0	13	249	255	96	7.2	8	250	306	96	10.7	10	249	437	95	17.3
6	249	320	95	13.6	11	298	231	99	1.2	6	299	403	96	11.9	9	300	252	94	12.8
5	300	420	96	13.4	10	349	335	94	16.3	5	349	304	97	8.2	8	349	393	94	17.7
3	348	412	94	18.0	9	399	564	98	8.5	3	400	493	96	14.3	6	448	564	90	46.7
2	399	536	92	32.6	8	450	825	99	8.1	2	449	356	93	19.1	5	499	521	95	18.8
1	451	630	91	47.4											4	549	275	88	28.0
															3	648	338	94	16.5
															2	798	387	93	23.0

B1–68 (seafloor: 400 m)					B5–60 (seafloor: 526 m)					B11–50 (seafloor: 3270 m)				
Niskin	Depth [m]	Ba_{xs} [pM]	Ba_{xs} [%]	Al [nM]	Niskin	Depth [m]	Ba_{xs} [pM]	Ba_{xs} [%]	Al [nM]	Niskin	Depth [m]	Ba_{xs} [pM]	Ba_{xs} [%]	Al [nM]
Transect B														
24	10	306	97	7.0	24	11	418	92	25.4	24	11	186	98	2.9
22	50	2761	100	6.9	22	51	286	93	16.5	20	99	134	100	0.4
18	74	2918	100	4.3	21	76	324	93	18.1	16	151	306	98	3.5
17	100	352	98	4.2	20	99	289	93	16.1	14	200	128	98	2.2
13	126	282	98	4.9	19	126	239	91	17.6	11	250	547	95	19.7
12	152	334	98	4.6	18	149	228	84	31.3	9	299	798	97	16.4
11	199	308	95	10.9	14	200	298	80	54.8	8	350	589	99	3.4
7	249	472	95	19.5	10	249	105	79	20.9	4	400	548	99	6.2
6	297	1013	96	31.9	9	299	556	88	57.3	3	453	458	99	3.6
					5	349	560	90	45.5					
					4	400	700	81	120.6					
					1	451	199	81	34.6					

C1–100 (seafloor: 140 m)					C5–91 (seafloor: 550 m)					C11–42 (seafloor: 3350 m)					C11–83 (seafloor: 3350 m)				
Niskin	Depth [m]	Ba_{xs} [pM]	Ba_{xs} [%]	Al [nM]	Niskin	Depth [m]	Ba_{xs} [pM]	Ba_{xs} [%]	Al [nM]	Niskin	Depth [m]	Ba_{xs} [pM]	Ba_{xs} [%]	Al [nM]	Niskin	Depth [m]	Ba_{xs} [pM]	Ba_{xs} [%]	Al [nM]
Transect C																			
24	10	596	23	1523	24	11	127	96	3.8	24	9	386	98	4.6	24	11	317	98	4.6
21	30	578	23	1420	22	50	130	95	4.6	21	49	370	98	4.5	20	50	218	96	7.0
17	49	552	20	1674	21	75	100	100	0.0	19	75	181	98	3.1	19	74	96	98	1.1
12	76	386	19	1221	20	100	162	96	4.9	17	98	241	98	4.2	18	99	218	97	4.9
10	102	359	13	1838	19	124	227	96	7.1	16	125	410	99	2.4	15	150	237	98	4.3
5	119	323	13	1573	18	149	422	95	15.0	14	150	234	99	1.4	13	249	450	98	5.4
4	131	573	20	1686	17	198	335	93	18.2	13	199	314	98	5.7	11	300	450	99	2.5
					16	250	423	88	42.4	12	250	503	98	8.2	9	349	528	99	2.9
					15	298	444	91	32.2	10	301	292	98	3.3	8	399	502	99	3.1
					14	348	505	95	18.8	8	400	221	98	2.7	7	449	1051	98	12.7
					13	398	557	98	8.3	7	450	368	98	6.7	5	548	357	99	2.4
					12	450	429	80	77.3	6	499	246	99	1.1	4	649	484	99	2.3
					1	498	403	81	68.2	5	550	688	97	17.0	3	798	431	98	6.2
										4	649	336	97	7.7					
										3	798	519	98	7.9					

greater depth around 1000 m (i.e. below the mesopelagic Ba_{xs} maximum) in various sectors of the S.O. (Cardinal et al., 2001, 2005; Jacquet et al., 2005) where input of Ba_{xs} as a result of export and remineralization is probably minimal, but where $BaSO_4$ saturation still prevails (Monnin et al., 1999; Monnin and Cividini, 2006). We therefore considered a Ba_{xs} value of 180 pM zone as representative of the Ba_{xs} background in the mesopelagic zone, in accordance with Dehairs et al. (1997). Proper assessment of residual Ba_{xs} signal, however, would require winter data, which at present are not available. For the assessment of mesopelagic POC remineralization from Ba_{xs} contents we assumed that the relationship given in Eq. (2) and established for the Atlantic sector of the S.O. south of the PF (Dehairs et al., 1997) applied for the present study area also located south of the PF. Standard errors on the POC remineralization rates calculated from the fitted Ba_{xs} values varied between 15% and 26%.

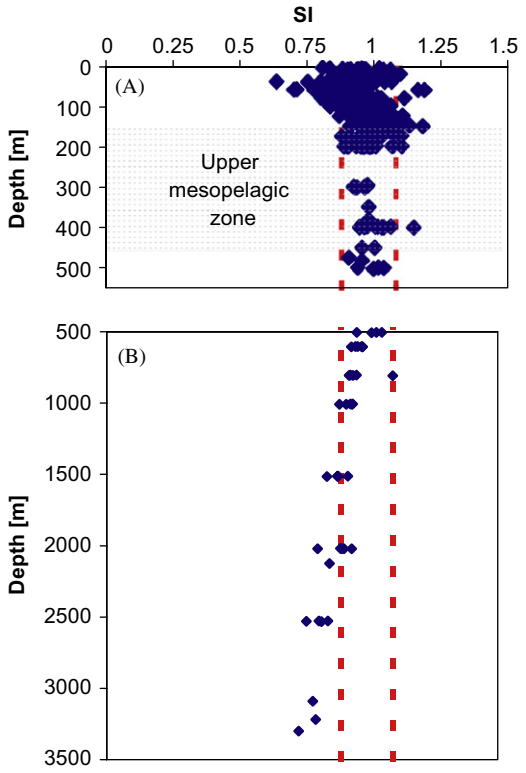

Fig. 2. Saturation index (SI) of pure barite in the upper 500 m water column (A) and between 500 and 3500 m (B). The vertical broken lines represent the saturation index value of 0.9 (left) and 1.1 (right).

3. Results

Particulate Ba_{xs} concentrations are reported in Table 1. At Plateau stations A3 and B1, Ba_{xs} concentrations in the upper 125 m were quite high (>1000 pM), while margin and off-shelf stations had Ba_{xs} concentrations ⩽400 pM (see the contrasting profiles in Figs. 3A and B at stations A3–119 and B11–50, respectively). The very high Ba_{xs} contents in the surface layer at A3 (up to 5900 pM; 50 m cast 73; Table 1) are quite unusual, though similar values were occasionally observed in earlier S.O. studies (Dehairs et al., 1992, 1997; Jacquet et al., 2007b). Furthermore, at A3 significant temporal changes in Ba_{xs} content occurred. Depth-weighted average (DWAv) concentrations (Table 2) of Ba_{xs} in the upper 125 m first increased from 578 (CTD 32; January 24th) to 4125 pM (CTD 73; February 3rd), but subsequently decreased to 2493 pM (CTD 119; February 12th).

The upper mesopelagic layer (125–450 m) at the margin and off-shelf stations (C5, C11, B5, and B11) shows the characteristic broad Ba_{xs} maximum (as illustrated in Fig. 3B for station B11–50), with concentrations reaching between 500 and 1050 pM at discrete depths (Table 1). Mesopelagic Ba_{xs} values exceeding 1000 pM have been recorded previously in the complex frontal region of the Crozet–Kerguelen Basin (Jacquet et al., 2005). While at station C11, DWAv Ba_{xs} values for the 125–450 m layer increased from 309 pM (CTD 42; January 26) to 493 pM (CTD 83; February 6) over a 10-day period, at station A3,

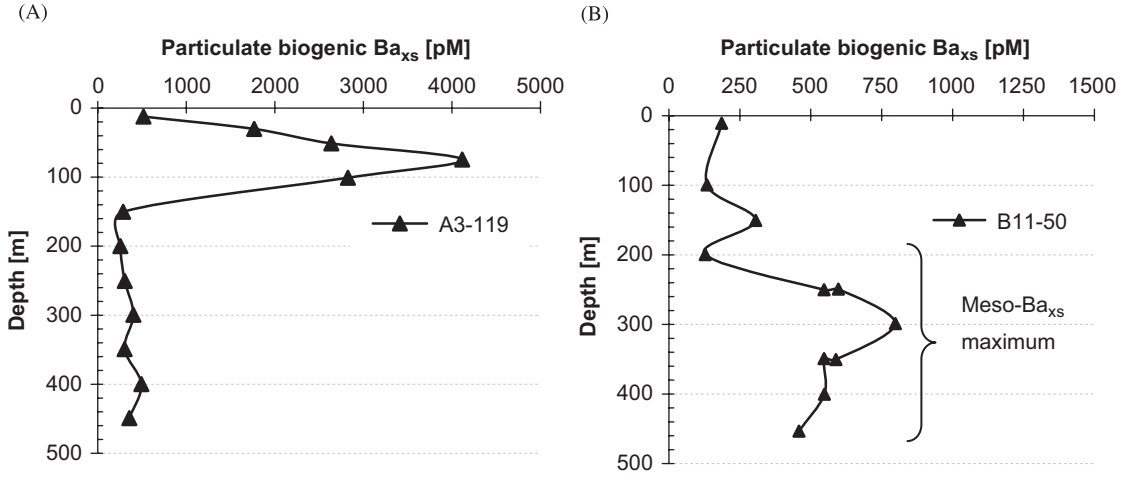

Fig. 3. Profiles of excess biogenic particulate Ba (Ba_{xs}; pM) at stations A3–119 and B11–50. Note the difference of scale between profiles.

Table 2
Depth-weighted average Ba_{xs} contents (pM) in the 0–125 m and the 125–450 m (= upper mesopelagic) depth layers

Station	Seafloor [m]	Ba_{xs} [pM]	
		0–125 m	125–450 m
A3_32	525	578	401
A3_73	525	4125	370
A3_119	525	2493	342
A11_11	2600	171	391
B1_68	400	1458	–
B5_60	526	322	403
B11_50	3270	157	474
C1_100	140	468	–
C5_91	550	140	447
C11_42	3350	315	309
C11_83	3350	219	493

Ba_{xs} contents remained rather stable over a 19-day period and even displayed a slight decrease from 401 pM (CTD 32; January 24) to 342 pM (CTD 119; February 12) (Table 2). The lowest and highest DWAv mesopelagic Ba_{xs} values during KEOPS were both observed at station C11 (309 and 493 pM for CTD 42 and 83, respectively). At station B11, the DWAv mesopelagic Ba_{xs} content also was quite high (474 pM), being only slightly lower than the value at station C11–83. Overall, it is interesting to note that the highest mesopelagic Ba_{xs} contents (>450 pM) were reached in off-shelf environments (C11 and B11), while margin and shelf environments demonstrated lower mesopelagic Ba_{xs} values ($\leqslant 400$ pM at all A3 casts and B5; C5 served as an exception, reaching ~450 pM). This is opposite to the situation in the upper 125 m layer, which demonstrated higher Ba_{xs} contents at Plateau stations compared to margin and off-shelf stations.

4. Discussion

4.1. Plateau vs. off-shelf environments

Primary production (PP) at A3 was high (864–1872 mg C m^{-2} d^{-1}) compared to C11 (216–384 mg C m^{-2} d^{-1}) (data from B. Griffith in Lefèvre et al., 2008), but at both these stations the bloom was mainly sustained by diatoms. These consisted of large cells at A3 and smaller cells at C11 (Armand et al., 2008). At A3, the Ba_{xs} signal in the upper 125 m during the different repeats (data in Tables 1 and 2) followed the variations in primary productivity, Chl_a and BSi variations (Mosseri et al., 2008). At Plateau stations, higher biological activities were reflected by the higher Ba_{xs} contents in the upper 125 m (stations A3 and B1), while at margin and off-shelf sites (stations C5, A11, B11, and C11) lower surface Ba_{xs} contents were in agreement with the lower biological activity at these sites. Based on scanning electron microscope–electron microprobe investigations, Stroobants et al. (1991) and Jacquet et al. (2007b) concluded that particulate Ba_{xs} in the surface waters is dispersed over different biogenic, non-barite phases (see also Cardinal et al., 2005) while in the mesopelagic water column, on the contrary, Ba_{xs} is mainly composed of discrete barite particles, as shown earlier by Dehairs et al. (1980). Though it is not yet totally clear how the surface and mesopelagic Ba_{xs} signals are linked, current understanding is that the mesopelagic Ba_{xs}, carried mainly by barite, is precipitated within $BaSO_4$-saturated micro-environments (i.e. aggregates, pellets), which are sulfate- and/or Ba-enriched because of the composition of the particles composing the micro-environment (Bishop, 1988), and/or which take up dissolved Ba up from the medium while sinking from the surface ML and degrading with time (Collier and Edmond., 1984; Dehairs et al., 2000; Jacquet et al., 2007a). Mesopelagic barite micro-crystals persist in $BaSO_4$ saturated waters, their stocks reflecting the intensity of the mesopelagic remineralization process (Dehairs et al., 1997).

Contrasting with the situation in the upper 125 m, our observations for the mesopelagic waters indicate that the off-shelf environments (stations C11–83 and B11) give rise to higher Ba_{xs} contents compared to the Plateau sites A3 and B5. Thus, the most intense mesopelagic remineralization appears to be taking place in the off-shelf environment. Our results furthermore suggest a significant increase of mesopelagic remineralization over time at off-shelf station C11, while at Plateau station A3 the system seems to evolve close to steady state.

4.2. Mesopelagic Ba_{xs} and bacterial production

Previous studies have highlighted the relationship between mesopelagic Ba_{xs} contents and OM remineralization (Dehairs et al., 1980, 1990, 1991, 1992, 1997; Ganeshram et al., 2003; Cardinal et al., 2005). Therefore, we expect mesopelagic Ba_{xs} content to be related with bacterial activity, as has recently been observed experimentally by Gonzalèz-Muñoz et al. (2003). During KEOPS, assessment of bacterial production was mostly limited to the upper 200 m (^{3}H-leucine method; Christaki et al., 2008), prohibiting a direct and systematic comparison with mesopelagic Ba_{xs} contents at all depths.

Bacterial carbon demand (BCD) calculated as BP/bacterial growth efficiency (using a mean BGE of 20% as reported for the upper 200 m at site A3–73; see Obernosterer et al., 2008) appears to follow closely euphotic zone integrated PP (Table 4). For the discussion on the comparison between PP and BCD we refer to the papers by Obernosterer et al. (2008) and Christaki et al. (2008). Rather than assessing the balance of the different carbon fluxes in the upper water column, our aim here is merely to investigate dependency of mesopelagic barite production on bacterial activity and also to weigh mesopelagic remineralization against carbon export from the surface. We assumed that vertical gradients of water-column-integrated BP in the upper 200 m could also possibly

provide information on the potential intensity of BP extent to depths exceeding 200 m. The underlying rationale is that steep, shallow gradients of water column integrated BP presumably indicate efficient, close to complete remineralization within the upper 200 m with relatively little OM left for consumption by bacteria deeper in the water column. On the contrary, weak gradients of integrated BP in the upper 200 m would indicate that significant bacterial activity is still ongoing at depths exceeding 200 m.

For KEOPS, we verified several regressions in order to check whether the depth to which significant BP extends is somehow related with the Ba_{xs} content in the upper mesopelagic (125–450 m) (Table 3). Depth-weighted (125–450 m) average mesopelagic Ba_{xs} was plotted vs. (1) height of the water column wherein 50% of the 200-m integrated BP takes place, and (2) ratio of integrated BP in the upper 200 m over integrated BP in the upper 125, 100, and 80 m and the ML. DWAv mesopelagic Ba_{xs} appears significantly correlated ($p<0.05$) with the height of the water column wherein 50% of the upper 200 m integrated BP occurs (see also Fig. 4A) and the ratio of 200 m over 125 (see also Fig. 4B), 100, and 80 m integrated BP. However, it is not significantly correlated with the ratio of 200 m over ML depth integrated BP (Table 3). These observations suggest indeed that systems where bacterial activity extends well below the mixed layer (i.e. high ratio of 200 m over 125, 100, and 80 m-integrated BP) are more efficiently exporting OM to greater depths for subsequent remineralization in the mesopelagic region. It is likely, however, that it is the general plankton community characteristics (e.g., species composition, cell sizes, phytoplankton biomass, biogenic material characterization, grazing, etc.) that define whether export of matter will be shallow or deep. Bacteria merely follow the food and their remineralization activity at mesopelagic depths tunes the Ba_{xs} formation. This scenario fits also with recent observations for the North Pacific (Dehairs et al., in press).

4.3. Mesopelagic C remineralization vs. PP, BCD, and EP

We translated Ba_{xs} DWAv into C fluxes using Eqs. (1) and (2), considering a residual Ba_{xs} content of 180 pM, i.e. the Ba_{xs} content in the absence of remineralization activity (see Experiment and method). The largest mesopelagic remineralization (up to 48 $mgC\,m^{-2}\,d^{-1}$) occurs in the less productive off-shelf region (stations C11–83 and B11), while the highly productive A3 site is characterized by lower remineralization rates (25 $mgC\,m^{-2}\,d^{-1}$ at A3–119; Table 4). Such remineralization fluxes are similar to those observed during summer in the PFZ in the Crozet–Kerguelen basin and along 145°E (Cardinal et al., 2005; Jacquet et al., 2005). In Table 4 we compare remineralization integrated over the 125–450-m-depth layer with PP integrated over the euphotic layer, BCD in the upper 200 m and export of carbon from the 125 m horizon. Ba_{xs}, PP, BCD, and EP were not always analyzed for the same CTD

Table 3
Correlations between mesopelagic Ba_{xs} contents and different expressions of gradients in bacterial production (BP) integrated over the upper 200 m water column (see text)

Linear regression ($y = b + ax$)	R^2	b	a	p
BP_{int} $Z = 50\%$ of BP_{int} 200 m vs. Meso-Ba_{xs}	0.712	0.709	0.152	0.0043
Ratio of BP_{int} 200 m over BP_{int} 125 m vs. Meso-Ba_{xs}	0.551	0.788	0.0010	0.0225
Ratio of BP_{int} 200 m over BP_{int}100 m vs. Meso-Ba_{xs}	0.452	0.764	0.0016	0.0474
Ratio of BP_{int} 200 m over BP_{int} 80 m vs. Meso-Ba_{xs}	0.539	0.711	0.0026	0.0242
Ratio of BP 200 m over/BP_{int} ML vs. Meso-Ba_{xs}	0.171	0.240	0.0047	0.2687*

*Not significant.

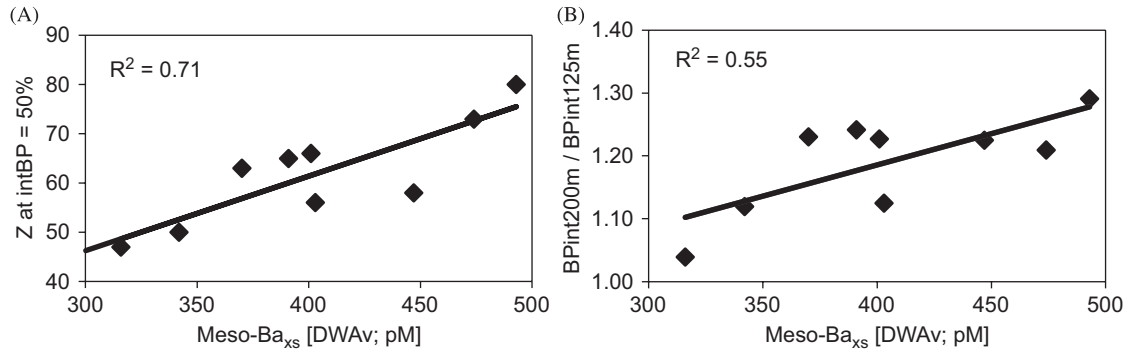

Fig. 4. (A) Regression of water-column height (Z; m) where 50% of the integrated bacterial production (BP) in the upper 200 m is achieved vs. depth weighted average (DWAv) mesopelagic excess particulate Ba (Ba_{xs} in pM); (B) regression of the ratio of upper 200 m integrated BP over upper 125 m integrated BP vs. depth weighted average (DWAv) mesopelagic Ba_{xs} (pM).

Table 4
Comparison of Ba_{xs}-based mesopelagic organic carbon remineralization with primary production (PP), bacterial carbon demand (BCD) and export production (EP); all fluxes in mg C m^{-2} d^{-1}

Station Ba cast	PP[a] *euphotic layer*	BCD[b] 0–200 m	EP[c] 125 m	Mesopelagic remin.[d] 125–450 m	Stnd error (%)	% Meso-remin.[d] vs. EP[c]
A3–32	1872	1705	264	34	17	13
A3–73	1644	830	223	29	19	13
A3–119	864	1005	266	25	22	9
A11–11	1400[e]	1170	216	32	18	15
B5–60	1250[e]	765	140	34	17	24
B11–50	250[e]	265	106	45	15	42
C5–91	350[e]	235	74	41	16	55
C11–42	384	340	114	21	26	18
C11–83	216	261	124	48	15	39

[a]PP, primary production; based on ^{14}C-incorporation (data from B. Griffith, in Lefèvre et al. (2008).
[b]BCD, bacterial carbon demand; from Obernosterer et al. (2008) and Christaki et al. (2008).
[c]EP, export production; based on ^{234}Th data; from Savoye et al. (2008).
[d]Mesopelagic remineralization, based on meso-Ba_{xs} data.
[e]PP based on ^{13}C-incorporation (data from N. Garcia, in Mosseri et al. (2008).

casts, but data were obtained for casts sampled close by in time and space. The off-shore site C11 shows the most drastic change over time, from lowest mesopelagic remineralization (21 mgC m^{-2} d^{-1}) on January 26 to highest (48 mg C m^{-2} d^{-1}) on February 6. This doubling of the remineralization at C11 was not paralleled by a similar change in PP, which remained relatively stable over the 10-day period.

Though ^{234}Th-based carbon export from the 125 m horizon is twice as large at A3 than at C11, export efficiency represents on average only ~18% of PP at A3 compared to an average of ~43% at C11 (Savoye et al., 2008 and Table 4). This observation implies that shallow (i.e. <125 m) remineralization is relatively more efficient above the Plateau. Such a non-linear response of carbon export relative to PP was attributed mainly to differences in efficiency of the microbial food web between on and off Plateau sites. Indeed, at C11, the transfer efficiency of primary produced biomass to higher trophic levels is enhanced via mesozooplankton grazing on the heterotrophic nanoplankton community (Christaki et al., 2008; Carlotti et al., 2008). Through fecal pellet production, such a condition likewise could sustain the relatively enhanced export production that is observed at C11. Also, on and off Plateau sites are quite different in remineralization efficiency of the carbon exported from the surface, which reached 18–39% at C11 compared to 9–15% at A3 (Table 4).

To summarize, on the Plateau a larger fraction of organic carbon that escapes shallow mineralization and is exported out of the upper 125 m, crosses the mesopelagic layer and probably reaches the seafloor at ~525 m, or is exported off-shelf. Thus, although the system above the Plateau is exporting in a less efficient manner compared to off-shelf, the transfer efficiency of the matter through the mesopelagic layer is larger above the Plateau (see Fig. 5). This scenario fits with the fact that larger diatoms (e.g., *Chaetoceros* spp. and *Eucampia antarctica*; Armand et al., 2008) are present at A3. Those cells that escape shallow remineralization would sustain fast and deep export, short-circuiting mesopelagic processing of OM. On the contrary at C11, small diatoms (e.g., *Fragilariopsis pseudonana*) were dominant (Armand et al., 2008) and would enhance potential for mesopelagic remineralization.

Overall, the combination of differences in diatom cell size and organization of microbial food web could explain the variability in meso-C remineralization fluxes and transfer efficiency through the mesopelagic zone between A3 and C11. This situation is probably shaped by the condition of Fe-repleteness above the Plateau (Blain et al., 2007). A similar situation was encountered during a recent iron-fertilization experiment (EIFEX; Open S.O.; Smetacek, 2005). Compared to natural blooms in HNLC waters, the Fe-induced bloom of EIFEX led to a lower C remineralized: export ratio (Jacquet et al., 2008). The C remineralized in the 150–1000 m depth layer during EIFEX accounted for around 11% of the surface export at 150 m (Jacquet et al., 2008), which is similar to the 9 to 13% range we report here at station A3 on Plateau (Table 4, see discussion above). This would suggest that materials exported from Fe-replete diatom-dominated blooms are effectively less prone to remineralization probably as a result of fast transfer of matter through the mesopelagic water column.

5. Conclusions

During the KEOPS cruise, the particulate biogenic Ba_{xs} distribution in the mesopelagic waters (125–450 m) appears closely tuned by bacterial activity in the overlying water column. The general picture emerging is that when BP extends deeper in the water column, as is the case for off-shelf sites, larger mesopelagic Ba_{xs} contents are observed, contrasting with situations where BP is mostly restrained to

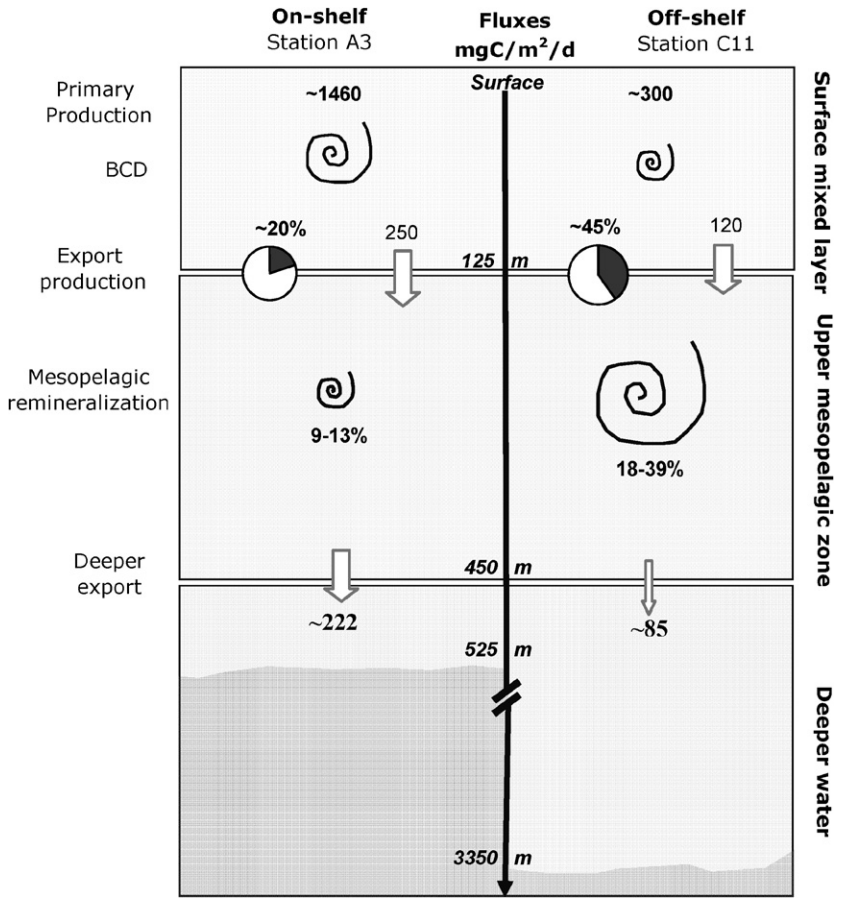

Fig. 5. Schematic, confronting the fate of organic carbon synthesized above the Plateau (station A3) and off-shelf (station C11). BCD = bacterial carbon demand.

a shallower surface layer, as is the case for the Plateau. With mesopelagic particulate Ba_{xs} reflecting OM remineralization, our findings indicate that the off-shelf open ocean east of the Kerguelen Plateau is a region of relatively more important intermediate water-column processing of exported matter, as compared to the Plateau. Thus, the fate of organic carbon exported from the upper water column of the Kerguelen Plateau area is quite different between the shelf region proper and the margin, open-ocean region. Indeed, though PP above the shelf area between Heard Island and Kerguelen is strongly boosted by a natural supply of iron, the fraction of PP exported from the upper 125 m is smaller for the shelf system as compared to the open-ocean system (Savoye et al., 2008). Furthermore, above the Plateau, the fraction of PP that escapes shallow (<125 m) remineralization and is exported out of the surface waters, appears less prone to subsequent remineralization in the mesopelagic depths. This could be the result of a faster transit of the sinking matter, probably because of the larger diatom cell size observed above the Plateau, which leaves less time for bacterial breakdown during transit of the matter through the deeper water column. It thus appears that the Fe-replete on-shelf system combines intensive shallow remineralization with a more efficient delivery of organic carbon below 450 m, while the Fe-depleted off-shelf HNLC system favors a more efficient export combined with more efficient mesopelagic remineralization (see Fig. 5). Overall, the twilight-zone C remineralization, as assessed by particulate biogenic Ba_{xs} stocks, appears to vary in response to changes in ecosystem and food web functioning. We advocate further studies focusing on the temporal variability of mesopelagic remineralization and its dependency on ecosystem structure for contrasting S.O. environments.

Acknowledgments

We thank the captain and crew of R.V. *Marion Dufresne* for their efficient assistance during work at sea. We are grateful to the chief scientists (S. Blain and B. Quéguiner; COM, France) and to colleagues who helped us during work on board. The skilful assistance of J. Navez and L. Monin (KMMA-MRAC, Tervuren) during sample processing and element analyses by ICP-AES and ICP-QMS in the home-based laboratory is greatly appreciated. This research was supported by the Federal Belgian Science Policy Office under SPSD Programmes on Global Change, Ecosystems and Biodiversity, Brussels, Belgium (BEL-

CANTO network contracts EV/37/7C, EV/03/7A, SD/CA/03A), the Vrije Universiteit Brussel under Grant GOA22 and the Research Foundation Flanders via contract G. 0021.04.

References

Aono, T., Yamada, Kudo, I., Imai, K., Nojiri, Y., Tsuda, A., 2005. Export fluxes of particulate organic carbon estimated from $^{234}Th/^{238}U$ disequilibrium during the Subarctic Pacific Iron Experiment for Ecosystem Dynamics Study (SEEDS 2001). Progress in Oceanography 64, 263–282.

Armand, L., Cornet-Barthau, V., Mosseri, J., Quéguiner, B., 2008. Late summer diatom biomass and community structure on and around the naturally iron-fertilized Kerguelen Plateau in the Southern Ocean. Deep-Sea Research II, this issue [doi:10.1016/j.dsr2.2007.12.031].

Aumont, O., Bopp, L., 2006. Globalizing results from ocean in situ iron fertilization studies. Global Biogeochemical Cycles 20, GB2017.

Biddanda, B., Benner, R., 1997. Major contribution from mesopelagic plankton to heterotrophic metabolism in the upper ocean. Deep-Sea Research 44, 2069–2085.

Bidigare, R.R., Hanson, K.L., Buesseler, K.O., Wakeham, S.G., Freeman, K.H., Pancost, R.D., Millero, F.J., Steinberg, P., Popp, B.N., Latasa, M., Landry, M.R., Laws, E.A., 1999. Iron-stimulated changes in ^{13}C fractionation and export by equatorial Pacific phytoplankton: Toward a paleogrowth rate proxy. Paleoceanography 14, 589–595.

Bishop, J.K.B., 1988. The barite-opal-organic carbon association in oceanic particulate matter. Nature 332, 341–343.

Bishop, J.K.B., Wood, T.J., Davis, R.E., Sherman, J.T., 2004. Robotic observations of enhanced carbon biomass and export at 55°S during SOFeX. Science 304, 417–420.

Blain, S., Tréguer, P., Belviso, S., Bucciarelli, E., Denis, M., Desabre, S., Fiala, M., Martin-Jézéquel, V., Le Fèvre, J., Mayzaud, P., Marty, J.C., Razouls, S., 2001. A biochemical study of the island mass effect in the context of the iron hypothesis, Kerguelen Islands, Southern Ocean. Deep-Sea Research I 48, 163–187.

Blain, S., Quéguiner, B., Armand, L., Belviso, S., Bombled, B., Bopp, L., Bowie, A., Brunet, C., Brussaard, C., Carlotti, F., Cristaki, U., Corbière, A., Durand, I., Ebersbach, F., Fuda, J.-L., Garcia, N., Gerringa, L., Griffiths, B., Guigue, C., Guillerm, C., Jacquet, S., Jeandel, C., Laan, P., Lefèvre, D., Lomonaco, C., Malits, A., Mosseri, J., Obernosterer, I., Park, Y-H., Picheral, M., Pondaven, P., Remenyi, T., Sandroni, V., Sarthou, G., Savoye, N., Scouarnec, L., Souhaut, M., Thuiller, D., Timmermans, K., Trull, T., Uitz, J., van-Beek, P., Veldhuis, M., Vincent, D., Viollier, E., Vong, L., Wagener, T., 2007. Effect of natural iron fertilization on carbon sequestration in the Southern Ocean. Nature 446, 1070–1074.

Boyd, P.W., Goldblatt, R., Harrison, P.J., 1999. Response of mesozooplankton to iron-enriched phytoplankton *n* the NE Subarctic Pacific. Deep-Sea Research II 46, 405–2432.

Boyd, P.W., Watson, A.J., Law, C.S., Abraham, E.R., Trull, T., Murdoch, R., Bakker, D.C.E., Bowie, A.R., Buesseler, K.O., Chang, H., Charette, M., Croot, P., Downing, K., Frew, R., Gall, M., Hadfield, M., Hall, J., Harvey, M., Jameson, G., LaRoche, J., Liddicoat, M., Ling, R., Maldonado, M.T., McKay, R.M., Nodder, S., Pickmere, S., Pridmore, R., Rintoul, S., Safi, K., Sutton, P., Strzepek, R., Tanneberger, K., Turner, S., Waite, A., Zeldis, J., 2000. Phytoplankton bloom upon mesoscale iron fertilisation of polar Southern Ocean waters. Nature 407, 695–702.

Boyd, P.W., Law, C.S., Wong, C.S., Nojiri, Y., Tsuda, A., Levasseur, M., Takeda, S., Rivkin, R., Harrison, P.J., Strzepek, R., Gower, J., McKay, R.M., Abraham, E., Arychuk, M., Barwell-Clarke, J., Crawford, W., Crawford, D., Hale, M., Harada, K., Johnson, K., Kiyosawa, H., Kudo, I., Marchetti, A., Miller, W., Needoba, J., Nishioka, J., Ogawa, H., Page, J., Robert, M., Saito, H., Sastri, A., Sherry, N., Soutar, T., Sutherland, N., Taira, Y., Whitney, F., Wong, S.K.E., Yoshimura, T., 2004. The decline and fate of an iron-induced Subarctic phytoplankton bloom. Nature 428, 549–553.

Broecker, W.S., Takahashi, T., Takahashi, T., 1985. Sources and flow patterns of deep-ocean waters as deduced from potential temperature, salinity and initial phosphate concentration. Journal of Geophysical Research 90, 6925–6939.

Buesseler, K.O., Andrews, J.E., Pike, S.M., Charette, M.A., 2004. The effect of iron fertilization on carbon sequestration in the Southern Ocean. Science 304, 414–417.

Buesseler, K.O., Andrews, J.E., Pike, S.M., Charette, M.A., Goldson, L.E., Brzezinski, M.A., Lance, V.P., 2005. Particle export during the Southern Ocean Iron Experiment (SOFeX). Limnology and Oceanography 50 (1), 311–327.

Buesseler, K.O., Lamborg, C.H., Boyd, P.W., Lam, P.J., Bishop, J.K.B., Casciotti, K.L., Dehairs, F., Elskens, M., Honda, M., Karl, D.M., Siegel, D., Silver, M.W., Steinberg, D.K., Trull, T.W., Valdes, J., Van Mooy, B., 2007. Revisiting carbon flux through the ocean's twilight zone. Science 316, 567–569.

Cardinal, D., Dehairs, F., Cattaldo, T., André, L., 2001. Constraints on export and advection in the Subantarctic and Polar Front Zones, south of Australia from the geochemistry of suspended particles. Journal of Geophysical Research 106, 31637.

Cardinal, D., Savoye, N., Trull, T.W., André, L., Kopczynska, E., Dehairs, F., 2005. Particulate Ba distributions and fluxes suggest latitudinal variations of carbon mineralization in the Southern ocean. Deep-Sea Research I 52, 355–370.

Carlotti, F., Thibault-Botha, D., Nowaczyk, A., Lefèvre, D., 2008. Zooplankton community structure, biomass and role in carbon fluxes during the second half of a phytoplankton bloom in the eastern sector of the Kerguelen shelf (January–February 2005). Deep-Sea Research II, this issue [doi:10.1016/j.dsr2.2007.12.010].

Christaki, U., Obernosterer, I., Van Wambeke, F., Veldhuis, M.J.W., Garcia, N., Catala, P., 2008. Microbial food web structure in a naturally iron fertilized area in the Southern Ocean (Kerguelen Plateau). Deep-Sea Research II, this issue [doi:10.1016/j.dsr2.2007.12.009].

Coale, K.H., Johnson, K.S., Fitzwater, S.E., Gordon, R.M., Tanner, S., Chavez, F.P., Ferioli, L., Sakamoto, C., Rogers, P., Millero, F., Steinberg, P., Nightingale, P., Cooper, D., Cochlan, W.P., Landry, M.R., Constantinou, J., Rollwagen, G., Trasvina, A., Kudela, R., 1996. A massive phytoplankton bloom induced by an ecosystem-scale iron fertilization experiment in the equatorial Pacific Ocean. Nature 383, 495–501.

Collier, R., Edmond, J., 1984. The trace element geochemistry of marine biogenic particulate matter. Progress in Oceanography 13, 113–199.

de Baar, H.J.W., Boyd, P.W., Coale, K.H., Landry, M.R., Tsuda, A., Assmy, P., Bakker, D.C.E., Bozec, Y., Barber, R.T., Brzezinski, M.A., Buesseler, K.O., Boyé, M., Croot, P.L., Gervais, F., Gorbunov, M.Y., Harrison, P.J., Hiscock, W.T., Laan, P., Lancelot, C., Law, C.S., Levasseur, M., Marchetti, A., Millero, F.J., Nishioka, J., Nojiri, Y., van Oijen, T., Riebesell, U., Rijkenberg, M.J.A., Saito, H., Takeda, S., Timmermans, K.R., Veldhuis, M.J.W., Waite, A.M., Wong, C.-S., 2005. Synthesis of iron fertilization experiments: from the Iron Age in the Age of Enlightenment. Journal of Geophysical Research 110, C09S16.

Dehairs, F., Chesselet, R., Jedwab, J., 1980. Discrete suspended particles of barite and the barium cycle in the open ocean. Earth and Planetary Science Letters 49, 40–42.

Dehairs, F., Goeyens, L., Stroobants, N., Bernard, P., Goyet, C., Poisson, A., Chesselet, R., 1990. On suspended barite and the oxygen minimum in the Southern Ocean. Global Biogeochemical Cycles 4, 85–102.

Dehairs, F., Stroobants, N., Goeyens, L., 1991. Suspended barite as a tracer of biological activity in the Southern Ocean. Marine Chemistry 35, 399–410.

Dehairs, F., Baeyens, W., Goeyens, L., 1992. Accumulation of suspended barite at mesopelagic depths and export production in the Southern Ocean. Science 258, 1332–1335.

Dehairs, F., Shopova, D., Ober, S., Veth, C., Goeyens, L., 1997. Particulate barium stocks and oxygen consumption in the Southern

Ocean mesopelagic water column during spring and early summer: relationship with export production. Deep-Sea Research II 44, 497–516.

Dehairs, F., Fagel, N., Antia, A.N., Peinert, R., Elskens, M., Goeyens, L., 2000. Export production in the Bay of Biscay as estimated from barium–barite in settling material: a comparison with new production. Deep-Sea Research I 47, 583–601.

Dehairs, F., Jacquet, S.H.M., Savoye, N., Bishop, J.K.B., van Mooy, B., Buesseler, K.O., Lamborg, C., Elskens, M., Boyd, P.W., Casciotti, K., Baeyens, W., in press. Barium in twilight zone suspended matter as a proxy for particulate organic carbon mineralization: results for the north pacific. Deep-Sea research II, topical issue on VERTIGO.

François, R., Honjo, S., Krishfield, R., Manganini, S., 2002. Factors controlling the flux of organic carbon to the bathypelagic zone of the ocean. Global Biogeochemical Cycles 16.

Ganeshram, R.S., François, R., Commeau, J., Brown-Leger, S.L., 2003. An experimental investigation of barite formation in seawater. Geochimica et Cosmochimica Acta 67, 2599–2605.

Gervais, F., Riebesell, U., Gorbunov, M.Y., 2002. Changes in primary productivity and chlorophyll *a* in response to iron fertilization in the southern Polar Frontal Zone. Limnology and Oceanography 47, 1324–1335.

Gonzalèz-Muñoz, M.T., Fernández-Luque, B., Martinez-Ruiz, F., Ben Chekroun, K., Arias, J.M., Rodriguez-Gallego, M., Martinez-Cañamero, M., de Linares, C., Paytan, A., 2003. Precipitation of barite by *Myxococcus xanthus*: possible implications for the biogeochemical cycle of barium. Applied and Environmental Microbiology 69 (9), 5722–5725.

Hoffmann, L.J., Peeken, I., Lochte, K., Assmy, P., Veldhuis, M., 2006. Different reactions of Southern Ocean phytoplankton size classes to iron fertilization. Limnology and Oceanography 51 (3), 1217–1229.

Hutchins, D.A., Bruland, K.W., 1998. Iron-limited diatom growth and Si:N uptake ratios in a coastal upwelling regime. Nature 393, 561–564.

Jacquet, S.H.M., Dehairs, F., Cardinal, D.B., Navez, J., Delille, B., 2005. Barium distribution across the Southern Ocean frontal system in the Crozet–Kerguelen Basin. Marine Chemistry 95, 149–310.

Jacquet, S.H.M., Dehairs, F., Savoye, N., Elskens, M., Cardinal, D.B., 2007a. Barium cycling along WOCE SR3 line in the Southern Ocean. Marine Chemistry 106, 33–45.

Jacquet, S.H.M, Henjes, J., Dehairs, F., Savoye, N., Maeyer-Vorobiec, A., Cardinal, D., 2007b. Particulate barium–barite and acantharians during the European Iron Fertilization Experiment (EIFEX) in the Southern Ocean. Journal of Geophysical Research—Biogeosciences, 112, G04006, doi:10.1029/2006JG000394.

Jacquet, S.H.M, Savoye, N., Dehairs, F., Strass, V., Cardinal, D., 2008. Mesopelagic C remineralization during the European Iron Fertilization Experiment (EIFEX). Global Biogeochemical Cycles, 22, GB1023, doi:10.1029/2006GB002902.

Kriest, I., Evans, G.T., 1999. Representing phytoplankton aggregates in biogeochemical models. Deep-Sea Research I 46, 1841–1859.

Lampitt, R.S., Antia, A.N., 1997. Particle flux in deep seas: regional characteristics and temporal variability. Deep-Sea Research I 44, 1377–1403.

Longhurst, A.R., Bedo, A.W., Harrison, W.G., Head, E.J.H., Sameoto, D.D., 1990. Vertical flux of respiratory carbon by oceanic diel migrant biota. Deep-Sea Research 37 (4), 685–694.

Lefèvre, D., Guigue, C., Obernosterer, I., 2008. The metabolic balance at two contrasting sites in the Southern Ocean: The iron-fertilized Kerguelen area and HNLC waters. Deep-Sea Research II, this issue [doi:10.1016/j.dsr2.2007.12.006].

Martin, J.H., 1990. Glacial–interglacial CO_2 change: the iron hypothesis. Paleoceanography 5, 1–13.

Martin, J.H., Fitzwater, S.E., 1988. Iron deficiency limits phytoplankton growth in the north-east Pacific Subarctic. Nature 331, 341–343.

Martin, J.H., Knauer, G.A., Karl, D.M., Broenkow, W.W., 1987. VERTEX: carbon cycling in the NE Pacific. Deep-Sea Research 34, 267–285.

Martin, J.H., Coale, K.H., Johnson, K.S., Fitzwater, S.E., Gordon, R.M., Tanner, S.J., Hunter, C.N., Elrod, V.A., Nowicki, J.L., Coley, T.L., Barber, R.T., Lindley, S., Watson, A.J., Van Scoy, K., Law, C.S., Liddicoat, M.I., Ling, R., Stanton, T., Stockel, J., Collins, C., Anderson, A., Bidigare, R., Ondrusek, M., Latasa, M., Millero, F.J., Lee, J., Yao, W., Zhang, J.Z., Friederich, G., Sakamoto, C., Chavez, F., Buck, K., Kolber, Z., Greene, R., Falkowski, P., Chisholm, S.W., Hoge, F., Swift, R., Yungel, J., Turner, S., Nightingale, P., Hatton, A., Liss, P., Tindale, N.W., 1994. Testing the iron hypothesis in ecosystems of equatorial Pacific Ocean. Nature 371, 123–129.

Monnin, C., Cividini, D., 2006. The saturation state of the world's ocean with respect to $(Ba,Sr)SO_4$ solid solutions. Geochimica et Cosmochimica Acta 70, 3290–3298.

Monnin, C., Jeandel, C., Cattaldo, T., Dehairs, F., 1999. The marine barite saturation state of the world's ocean. Marine Chemistry 65, 253–261.

Mosseri, J., Quéguiner, B., Armand, L., Cornet-Barthaux, V., 2008. Impact of iron on silicon utilization by diatoms in the Southern Ocean: A case of Si/N cycle decoupling in a naturally iron-enriched area. Deep-Sea Research II, this issue [doi:10.1016/j.dsr2.2007.12.003].

Nodder, S.D., Waite, A.M., 2001. Is Southern Ocean organic carbon and biogenic silica export enhanced by iron-stimulated increases in biological production? Sediment trap results from SOIREE. Deep-Sea Research II 48, 2681–2701.

Nodder, S.D., Charette, M.A., Waite, AM., Trull, T.W., Boyd, P.W., Zeldis, J., Buesseler, K.O., 2001. Particle transformations and export flux during an in situ iron-stimulated algal bloom in the Southern Ocean. Geophysical Research Letters 28, 2409–2412.

Obernosterer, I., Christaki, U., Lefèvre, D., Catala, P., Van Wambeke, F., Le Baron, P., 2008. Rapid bacterial remineralization of organic carbon produced during a phytoplankton bloom induced by natural iron fertilization in the Southern Ocean. Deep-Sea Research II, this issue [doi:10.1016/j.dsr2.2007.12.005].

Park, Y.H., Fuda, J.L., Durand, I., Naveira Garabato, A.C., 2008a. Internal tides and vertical mixing over the Kerguelen Plateau. Deep-Sea Research II, this issue [doi:10.1016/j.dsr2.2007.12.027].

Park, Y.H., Roquet, F., Durand, I., Fuda, J.L., 2008b. Large scale circulation over and around the Northern Kerguelen Plateau. Deep-Sea Research II, this issue [doi:10.1016/j.dsr2.2007.12.030].

Passow, U., De La Rocha, C.L., 2006. Accumulation of mineral ballast on organic aggregates. Global Biogeochemical Cycles 20, GB1013.

Reinthaler, T., van Aken, H., Veth, C., Arístegui, J., Robinson, C., Williams, P., Lebaron, P., Herndl, G., 2006. Prokaryotic respiration and production in the meso- and bathypelagic realm of the eastern and western North Atlantic basin. Limnology and Oceanography 51 (3), 1262–1273.

Sarmiento, J.L., Slater, R.D., Fasham, M.J.R., Ducklow, H.W., Toggweiler, J.R., 1993. A seasonal three-dimensional ecosystem model of nitrogen cycling in the North Atlantic photic zone. Global Biogeochemical Cycles 7, 417–450.

Sarmiento, J.L., Gruber, N., Brzezinski, M.A., Dunne, J.P., 2004. High-latitude controls of thermocline nutrients and low-latitude biological productivity. Nature 427, 56–60.

Savoye, N., Trull, T.W., Jacquet, S., Navez, J., Dehairs, F., 2008. 234Th-based export fluxes during a natural iron fertilisation experiment in the southern ocean. Deep-Sea Research II, this issue [doi:10.1016/j.dsr2.2007.12.036].

Shopova, D., Dehairs, F., Baeyens, W., 1995. A simple model of biogeochemical element distribution in the oceanic water column. Journal of Marine Systems 6, 331–344.

Smetacek, V., 2005. Fahrtabschnitt ANT XXI/3 Kapstadt-Kapstadt (21.01.04–25.03.04), 1. Introduction. Reports on Polar and Marine Research 500, 3–7.

Stroobants, N., Dehairs, F., Goeyens, L., Vanderheijden, N., Van Grieken, R., 1991. Barite formation in the Southern Ocean water column. Marine Chemistry 35, 411–422.

Suess, E., 1980. Particulate organic carbon flux in the ocean-surface productivity and oxygen utilization. Nature 280, 260–263.

Takeda, S., 1998. Influence of iron availability on nutrient consumption ratio of diatoms in oceanic waters. Nature 393, 774–777.

Taylor, S.R., McLennan, S.M., 1985. The continental crust: its composition and evolution. Blackwell Scientific Publications, Oxford, 312pp.

Trull, T.W., Armand, L., 2001. Insights into Southern Ocean carbon export from the $\delta^{13}C$ of particles and dissolved inorganic carbon during the SOIREE iron fertilisation experiment. Deep-Sea Research II 48, 2655–2680.

van Beek, P., Bourquin, M., Reyss, J.L., Souhault, M., Charette, M., Jeandel, C., 2008. Radium isotopes to investigate the water mass pathways on the Kerguelen Plateau (Southern Ocean). Deep-Sea Research II, this issue [doi:10.1016/j.dsr2.2007.12.025].